Ambipolar magnetic fluctuation-induced heat transport in toroidal devices*

P. W. Terry,† G. Fiksel, H. Ji,[a] A. F. Almagri, M. Cekic, D. J. Den Hartog,
P. H. Diamond,[b] S. C. Prager, J. S. Sarff, W. Shen, M. Stoneking,
and A. S. Ware
Department of Physics, University of Wisconsin—Madison, Madison, Wisconsin 53706

(Received 10 November 1995; accepted 4 January 1996)

The total magnetic fluctuation-induced electron thermal flux has been determined in the Madison Symmetric Torus (MST) reversed-field pinch [Fusion Technol. **19**, 131 (1991)] from the measured correlation of the heat flux along perturbed fields with the radial component of the perturbed field. In the edge region the total flux is convective and intrinsically ambipolar constrained, as evidenced by the magnitude of the thermal diffusivity, which is well approximated by the product of ion thermal velocity and the magnetic diffusivity. A self-consistent theory is formulated and shown to reproduce the experimental results, provided nonlinear charge aggregation in streaming electrons is accounted for in the theory. For general toroidal configurations, it is shown that ambipolar constrained transport applies when remote magnetic fluctuations (i.e., global modes resonant at distant rational surfaces) dominate the flux. Near locations where the dominant modes are resonant, the transport is nonambipolar. This agrees with the radial variation of diffusivity in MST. Expectations for the tokamak are also discussed. *© 1996 American Institute of Physics.* [S1070-664X(96)91505-8]

I. INTRODUCTION

The motion of charged particles along the stochastic fields of magnetic turbulence is generally regarded as an important transport mechanism in fusion and astrophysical plasmas. Because the rates of streaming along magnetic fields are greatly different for electrons and ions of comparable temperature, electron and ion loss rates are not necessarily ambipolar (i.e., equal) as they are for electrostatic turbulence. For particle transport, the fluxes are constrained by Ampère's law to be ambipolar for localized, internally generated fluctuations, independent of the value of the spatial mean electric field.[1] The same self-consistency constraint, however, does not lead to intrinsic ambipolarity in the heat flux, either under quasilinear theory,[1] or under more realistic renormalized theories of the turbulent response.[2,3] This difference is attributed to the fact that the electromagnetic potentials of ambipolarity are created in response to, and ultimately control, charge densities. They cannot distinguish between events that interchange two particles of disparate energies from those that interchange particles of equal energy.[3] Such arguments imply that the electron heat loss is tied to the electron thermal velocity, whereas the particle loss is tied to the slower ion thermal velocity. This leads to a marked disparity in the rates of convective and conductive heat loss.[4]

We describe herein experimental observations and an analytical theory that directly contradict the above assertions. Measurement of the magnetic fluctuation-induced electron heat flux[5] in the edge of the Madison Symmetric Torus[6] (MST) shows that it is convective, despite the presence of a temperature gradient, and ambipolar constrained. The ambipolar constraint is underscored by a simple modeling exercise that shows that the flux is well described by a Rechester–Rosenbluth diffusivity,[7] but with ion thermal velocity as the streaming factor. In the theory, ambipolar constraints are shown to arise through nonlinear bunching of electrons and the effect of this bunching on the collective plasma dielectric response through resonant momentum and energy exchanges. When the ions of the dielectric response are adiabatic (i.e., their thermal velocity exceeds the fluctuation phase velocity), the edge electron heat flux is convective, manifestly ambipolar constrained, and agrees well with the measurement in terms of its magnitude and scaling.

The electron bunching crucial in present considerations is not accounted for in conventional theories of turbulence.[8] This bunching arises from correlations among streaming electrons, whose relative separations lie within a correlation length of the scattering fields. Such electrons remain correlated for sufficiently long to act as discrete clumps of ballistically propagating electrons. The moving clumps induce a shielding response in the plasma dielectric, causing a transfer of energy and momentum to the fields through *resonant* emission. The excited fields, in turn, transfer energy back to the distributions via Landau damping, a process governed by the identical resonance condition. The self-consistent momentum and energy exchange between electrons and electrons and ions, as mediated by the turbulent fields, is thus elastic. Consequently, the turbulent collisions behave like Coulomb collisions, with scattering between isothermal particles of the same species producing no transport. In a self-consistent treatment of collisionless magnetic turbulence involving no temperature gradients, this constraint was found to eliminate transport involving turbulent electron–electron scattering, the type described by quasilinear theory.[9] In that treatment, it was also assumed that the residual ambipolar constrained losses due to turbulent electron–ion collisions are negligibly small. This led to the conclusion that electro-

*Paper 7Q10, Bull. Am. Phys. Soc. **40**, 1816 (1995).
†Invited speaker.
[a]Present address: Princeton Plasma Physics Laboratory, Princeton, New Jersey 08543.
[b]Department of Physics, University of California at San Diego, La Jolla, California 92093.

static fluctuations alone regulate transport. Here, in contrast, the temperature gradient allows the existence of a quasilinear-like conductive flux associated with turbulent electron–electron transfer. This flux arises from the perpendicular energy moment. As with field-aligned momentum,[10] there is no transport of parallel energy via turbulent electron–electron collisions. The ambipolar-constrained flux due to turbulent electron–ion collisions has both convective and conductive components and is not necessarily small. For MST parameters in the edge, the convective flux dominates both its conductive counterpart and the nonambipolar electron–electron flux. In this case, magnetic turbulence regulates transport, but in a way that is ambipolar constrained.

II. EXPERIMENT

The magnetic fluctuation-induced electron thermal flux was measured in MST,[6] a large reversed-field pinch (RFP) with a minor radius of $a=0.52$ m, a major radius of $R=1.5$ m, and a plasma current of $I<0.7$ MA. Plasmas in MST typically have a line-average density and temperature of $1\times10^{13}\ \mathrm{cm}^{-3}$ and 300 eV, respectively. Limited profile diagnostics [four-chord far infrared (FIR) and Thompson scattering] indicate that density and temperature profiles are broad but not flat. The density profile tends to peak more than the temperature profile, particularly at lower densities. The plasma core typically rotates. The impurity ion rotation speed is 10^4 m/s; the main plasma ion rotation speed is not measured. However, correlation between impurity ion slowing down and mode rotation rate decrease before and during sawtooth crashes suggests that impurity and main plasma ion rotation rates are similar.[11] Although the rotation profile is not known in MST, a decrease of rotation rate with radius is implied by the lack of rotation beyond the reversal layer.

MST discharges are characterized by a broad spectrum of magnetic turbulence. Magnetic fluctuations are measured both by insertable probes and by extensive wall-mounted probe arrays. Power is concentrated in the low frequencies ($\upsilon\leqslant20$ kHz), where fluctuations are of the order of a percent ($\tilde{B}/B_0\approx0.01$) and helicities correspond to $m=1$, $n=5$–8. At higher frequencies the fluctuation spectrum obeys a power law (decaying as $\omega^{-5/2}$) and encompasses higher helicities.[12] In the high-frequency range, the toroidal wave number varies linearly with frequency, with frequencies from 50–200 kHz corresponding to toroidal mode numbers from 30–70. These measurements indicate that even at the edge, magnetic turbulence is dominated by fluctuations whose resonant surface lies well in the core. Extensive numerical modeling studies[13] have established that the low-frequency spectrum component corresponds to internally resonant nonlinearly saturated global tearing modes. These modes are responsible for sustaining the reversal of the mean toroidal magnetic field, but in so doing they stochasticize the magnetic field within the reversal radius.[14] Simulations also indicate that they interact quasicoherently, giving rise to a spectrum that is nonstationary at low wave number. The temporal evolution of the magnetic field for the dominant modes ($n=5$–8) indicates a broad spectrum with signatures due to sawtoothing at 1 kHz, a 10 kHz signal associated with rotation of the $n\approx6$ modes at the plasma rotation speed, and a high-frequency tail.[15] At least some of the high-frequency signal is believed to result from aliasing effects with shorter-wavelength fluctuations. For a fixed wave number in the range of the dominant tearing modes, the frequency spectrum is dominated by rotation and quite coherent. The width of the frequency spectrum (half-width at half-maximum) is no greater than one-quarter the value of the peak. A peak at very low frequency due to sawtoothing appears as a distinct feature. Magnetic probe array measurements indicate that the electron mean-free path is many times larger than the parallel correlation length.

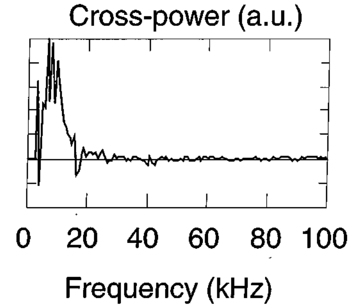

FIG. 1. Cross-power spectrum for the correlation of the fluctuating parallel heat flux with the fluctuating radial magnetic field for $r/a=0.75$.

Measurements of the magnetic fluctuation-induced heat and particle fluxes have been reported previously.[5,12] The particle flux Γ_e was obtained using an electrostatic energy analyzer in conjunction with a magnetic probe to correlate the parallel electron current fluctuation with $\tilde{B}_r$. The heat flux Q_e was obtained with a fast pyrobolometer and magnetic probe to correlate the fluctuating parallel heat flux with $\tilde{B}_r$. Both measurements covered a region from $r/a=0.8$ to the wall. The toroidal field reverses sign at $r/a\approx0.85$–0.9. The cross power of parallel heat flux and $\tilde{B}_r$ is shown in Fig. 1. The cross power peaks at 10 kHz with virtually all of the power below 20 kHz. From the dispersion curve for the toroidal mode number, this frequency range is identified with the global tearing modes ($n=5$–8). The absence of any significant contribution from higher-frequency fluctuations will be an important element of later analysis. A comparison of the convective heat flux, $\frac{3}{2}\Gamma_e T_e$, calculated from the measured magnetic fluctuation-induced particle flux, and the measured magnetic fluctuation-induced total heat flux Q_e is shown in Fig. 2 as a function of radius in the outer region of the plasma. Bounds on an estimate of the total electron heat flux inferred from a global power balance are indicated by the hatched region. Figure 2 shows that Q_e accounts for all thermal losses at $r/a=0.8$. Closer to the wall, however, Q_e drops sharply, becoming much smaller than the power balance-inferred heat flux. This is consistent with stochasticity ending at the reversal layer (in the region $r/a\approx0.85$–0.9) and some other mechanism (e.g., electrostatic fluctuations) driving the heat flux in the edge. Figure 2 indicates that Q_e is convective over the entire range sampled. This observation invalidates the inequality $\alpha_e\equiv Q_e/\Gamma_e T_e>5$ as a signature that transport is dominated by magnetic braiding.[4] A value of α_e greater than unity would occur if the total heat flux were not ambipolar constrained while the convective flux were.

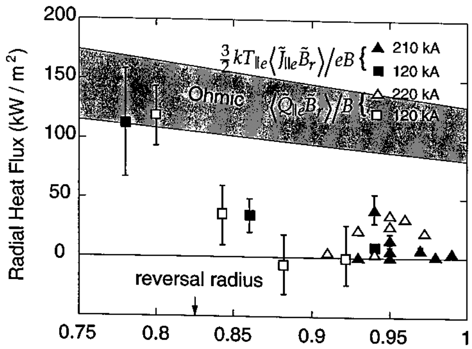

FIG. 2. Total magnetic fluctuation-induced electron thermal flux and convective thermal flux as a function of radius from $r/a \approx 0.8$ outward. The shaded region indicates the magnitude of the total heat flux inferred from a power balance.

The inference from Fig. 2 is that ambipolar constraints apply to the total heat flux Q_e. This is further illustrated by comparing the results of Fig. 2 with the Rechester–Rosenbluth model, $Q_{eR} = v_e(\tilde{B}/B_0)^2 L_\parallel$. Using the spectrum-averaged magnetic fluctuation power ($\tilde{B}/B_0 \approx 0.01$) and a parallel correlation length ($L_\parallel \approx 1$ m) known approximately from magnetic probe array measurements to within a factor of 2–3, this expression agrees with the results of Fig. 2, *but only if the electron thermal velocity is replaced by the ion thermal velocity*. Otherwise it is off by over an order of magnitude.

III. THEORY

In light of these measurements, we calculate the Lenard–Balescu turbulent collision integral (LBTCI),[9] in order to evaluate the electron heat flux moment of the fluctuating electron distribution for an equilibrium with temperature and density gradients. The electron heat flux is

$$Q_e = \mathrm{Re} \int d^3v \, \frac{m_e v^2}{2} \sum_{k,\omega} \frac{ic}{B_0} \mathbf{k} \times \mathbf{b}_0 \cdot \hat{r} \times \left\langle \left[\phi - \frac{v_\parallel}{c} A_\parallel \right] h_e \right\rangle_{k,\omega}, \tag{1}$$

where ϕ and $A_\parallel$ are the electrostatic and magnetic potentials, h_e is the nonadiabatic part of the electron distribution, $\mathbf{b}_0$ is the unit vector along the equilibrium magnetic field, and $\hat{r}$ is the radial unit vector. This expression describes $E \times B$ advection of heat, and heat loss via electron streaming along the perturbed magnetic field $\tilde{B} = \nabla A_\parallel \times \mathbf{b}_0$. The component of Q_e proportional to $A_\parallel$ yields the heat flux measured by experiment.

The electron distribution appearing in Eq. (1) is obtained from the electron drift kinetic equation (DKE),

$$\frac{\partial h_e}{\partial t} + v_\parallel \nabla_\parallel h_e + v_\parallel \frac{\nabla A_\parallel \times \mathbf{b}_0}{B_0} \cdot \nabla_\perp h_e - \frac{c}{B_0} \nabla \phi \times \mathbf{b}_0 \cdot \nabla_\perp h_e = -\sum_{\mathbf{k}} \frac{|e| \langle f_e \rangle}{T_e} i(\omega - \omega_*^T) \left(\phi_{\mathbf{k},\omega} - \frac{v_\parallel}{c} A_{\parallel \mathbf{k},\omega} \right) \times \exp(i\omega t - i\mathbf{k} \cdot \mathbf{x}), \tag{2}$$

where $\omega_{*e}^T = (cT_e/eB_0)\mathbf{k} \times \mathbf{b}_0 \cdot \hat{r} L_n^{-1}[1 + \eta_e(v^2/v_e^2 - \frac{3}{2})]$ is the diamagnetic frequency, $\eta_e = L_{ne}/L_{Te}$ is the ratio of density gradient scale length to temperature gradient scale length, v_e is the electron thermal velocity, and $\langle f_e \rangle$ is the equilibrium distribution function.

The solution of the DKE has the form

$$h_e(\mathbf{k},\omega) = R_\phi(\mathbf{k},\omega)\phi_{\mathbf{k},\omega} + R_A(\mathbf{k},\omega) A_{\parallel \mathbf{k},\omega} + \tilde{h}_e(\mathbf{k},\omega), \tag{3}$$

where the first two terms are referred to as the coherent response, representing the response of the distribution to potential disturbances at the same wave number and frequency, and the third term is the incoherent distribution. In a moderate to weak turbulence regime where resonance broadening effects are of second order, the coherent responses are given by

$$R_\phi(\mathbf{k},\omega) = -i \frac{(\omega - \omega_*^T)}{(\omega - k_\parallel v_\parallel)} e \langle f_e \rangle / T_e \tag{4}$$

and

$$R_A(\mathbf{k},\omega) = -\frac{v_\parallel}{c} R_\phi(\mathbf{k},\omega). \tag{5}$$

The neglect of resonance broadening effects is consistent with the narrow spectrum at low wave number, as described in the previous section. The incoherent distribution $\tilde{h}_e(\mathbf{k},\omega)$ arises from the nonlinear coupling. In Fourier space, the nonlinearities of Eq. (2) are convolutions, allowing $h_e(k,\omega)$ to be driven by potential amplitudes at different $\mathbf{k}$ and ω. The structure and dynamical properties of the incoherent distribution are obtained from the solution of the evolution equation[8] for the two-point phase space density correlation $\langle h_e(\mathbf{x}_1,\mathbf{v}_1,t) h_e(\mathbf{x}_2,\mathbf{v}_2,t) \rangle$. The incoherent distribution is identified with correlated electron clumps that propagate ballistically along the equilibrium magnetic field. The spatial and temporal properties of the incoherent distribution make it distinct from the plasma dielectric. Specifically, quasineutrality and Ampère's law describe the shielding of the clumps by the dielectric. The shielding relationship is implicit in the structure of Eq. (3): the response functions R_A and R_ϕ are electron susceptibilities that contribute to the dielectric in the usual way. The incoherent distribution, however, is not proportional to $\phi_{\mathbf{k}}$ or $A_{\parallel \mathbf{k}}$, and does not contribute to the dielectric. The shielding of the particle-like clump is analogous to the shielding of moving test particles by a plasma dielectric.

Substituting the electron distribution, Eq. (3), into the heat flux, Eq. (1), leads to the LBTCI,

$$Q_e = \mathrm{Re} \int d^3v \, \frac{m_e v^2}{2} \sum_{k,\omega} \frac{ic}{B_0} \mathbf{k}\times\mathbf{b}_0 \cdot \hat{r} \Bigg(-\frac{v_\parallel}{c} R_A(\mathbf{k},\omega) \times \langle A_\parallel A_\parallel \rangle_{\mathbf{k},\omega} - \frac{v_\parallel}{c} \langle A_\parallel \tilde{h}_e \rangle_{\mathbf{k},\omega} + R_\phi(\mathbf{k},\omega) \langle \phi\phi \rangle_{\mathbf{k},\omega} + \langle \phi \tilde{h}_e \rangle_{\mathbf{k},\omega} + R_A(\mathbf{k},\omega) \langle \phi A_\parallel \rangle_{\mathbf{k},\omega} - \frac{v_\parallel}{c} R_\phi(\mathbf{k},\omega) \times \langle A_\parallel \phi \rangle_{\mathbf{k},\omega} \Bigg). \tag{6}$$

In this expression, the coherent and incoherent components of the distribution play roles consistent with those played in the constituitive relations. The coherent responses, through the gradient dependence of R_A and R_ϕ, produce diffusive terms when the divergence of the flux is taken. If the coherent response to the magnetic potential is linearized, the diffusivity is that of quasilinear theory with a Rechester–Rosenbluth-like scaling. Similar scaling also follows when a nonlinear (resonance broadened) coherent response is used.[3] The incoherent distribution leads to a drag-like term in the LBTCI. The ballistically propagating electron correlations are shielded by the plasma dielectric, inducing emission into the collective modes of the dielectric in the form of a resonant exchange of momentum and energy between macroparticle and modes. This emission process subjects the clump to a drag.

The shielding and drag processes enter Eq. (6) when the transport description is made self-consistent by relating the potentials to the charge distributions through Ampère's law and quasineutrality. These constraints are given, respectively, by

$$\frac{4\pi e}{c} \int d^3v \; v_\parallel [F_i - R_\phi(\mathbf{k},\omega)\phi_{\mathbf{k},\omega} - R_A(\mathbf{k},\omega) A_{\parallel\mathbf{k},\omega} - \tilde{h}_e(\mathbf{k},\omega)] = -k^2 A_{\parallel\mathbf{k},\omega} \tag{7}$$

and

$$4\pi e \int d^3v [F_i - R_\phi(\mathbf{k},\omega)_{\mathbf{k},\omega} - R_A(\mathbf{k},\omega) A_{\parallel\mathbf{k},\omega} - \tilde{h}_e(\mathbf{k},\omega)] = 0, \tag{8}$$

where $F_i = -\langle f_i \rangle e\phi/T_i + h_i$ is the full ion distribution, h_i is the nonadiabatic ion distribution, satisfying $(\omega - k_\parallel v_\parallel) h_i(k) = (\omega - \omega_{*i}^T)\langle f_i \rangle J_0(k_\perp v_\perp/\Omega_i)(e/T_i)(\phi_{\mathbf{k},\omega} - v_\parallel c^{-1} A_{\parallel\mathbf{k},\omega})$, $\omega_{*i}^T = -\omega_{*e}^T(e\rightarrow i)$, J_0 is the zeroth-order Bessel function, and Ω_i is the ion gyrofrequency. Note that the ion and coherent electron distributions are compatible with shielding of tearing mode current layers by outer tearing eigenmode structures on neighboring rational surfaces in a finite ω_* kinetic description. However, parts of these distributions also go beyond simple tearing mode physics. The nonadiabatic ions, for example, provide the dissipative electron–ion coupling that ultimately governs the ambipolar-constrained parts of the flux.

Ampère's law and quasineutrality are imposed on Eq. (6) by solving Eqs. (7) and (8) for $A_{\parallel\mathbf{k},\omega}$ and $\phi_{\mathbf{k},\omega}$ and substituting into Eq. (6). In the resulting expression, the magnetic drag term, $\langle A_\parallel \tilde{h}_e \rangle_{\mathbf{k},\omega}$, becomes a linear combination of the correlations $\langle \tilde{n}_e \tilde{h}_e \rangle_{\mathbf{k},\omega}$ and $\langle \tilde{J}_\parallel \tilde{h}_e \rangle_{\mathbf{k},\omega}$, where $\tilde{J}_\parallel = |e| \int d^3v \; v_\parallel \tilde{h}_e$ and $\tilde{n}_e = \int d^3v \; h_e$ are the incoherent current and density terms of Ampère's law and quasineutrality. The magnetic diffusion term, $\langle A_\parallel A_\parallel \rangle_{\mathbf{k},\omega}$, becomes a linear combination of the $\int d^3v$ and $\int d^3v \; v_\parallel$ moments of the correlations $\langle \tilde{J}_\parallel \tilde{h}_e \rangle_{\mathbf{k},\omega}$ and $\langle \tilde{n}_e \tilde{h}_e \rangle_{\mathbf{k},\omega}$. Solutions of the two-point evolution equation indicate[8] that the correlations $\langle \tilde{J}_\parallel \tilde{h}_e \rangle_{\mathbf{k},\omega}$ and $\langle \tilde{n}_e \tilde{h}_e \rangle_{\mathbf{k},\omega}$ are ballistic in character, allowing the two-time two-point correlations to be written in terms of one-time two-point correlations, as

$$\langle \tilde{K} \tilde{h}_e \rangle_{\mathbf{k},\omega} = 2\pi \delta(\omega - k_\parallel v_\parallel) \langle \tilde{K} \tilde{h}_e \rangle_{\mathbf{k}}, \tag{9}$$

where $\tilde{K}$ is either $\tilde{n}_e$ or $\tilde{J}_\parallel$. These constraints impose on the emission process and resulting drag force the same resonant condition that characterizes the damping of wave energy and ultimately leads to diffusion. As a consequence, these constraints produce a partial cancellation of the diffusion with the drag, considerably simplifying the LBTCI. Ampère's law and quasineutrality are then used to rewrite the correlations of incoherent fluctuations in terms of power densities $\langle |A_\parallel|^2 \rangle_{k,\omega}$ and $\langle |\phi|^2 \rangle_{k,\omega}$. The algebraic procedure described above is straightforward but tedious. Because it has been detailed elsewhere[9] we do not repeat the steps here.

Following the above steps, the LBTCI can be written as

$$Q_e = \left[-v_e D_{\nabla T}^{(e-e)} \frac{1}{L_{Te}} - v_i \left(D_{\nabla n}^{(e-i)} \frac{1}{L_{ni}} + D_{\nabla T}^{(e-i)} \frac{1}{L_{Ti}} \right) \right] n_0 T_e, \tag{10}$$

where, for sake of comparison with experiment, only the magnetic components have been displayed. In this expression, $D_{\nabla T}^{(e-e)}$ is the diffusivity of the conductive heat flux of quasilinear theory and $D_{\nabla n}^{(e-i)}$ and $D_{\nabla T}^{(e-i)}$ describe transport produced by the momentum and energy exchange between electron clumps and ions as mediated by collective modes. The diffusivity of the conductive heat flux comes from the temperature gradient-dependent parts of the coherent electron response, and is given by

$$D_{\nabla T}^{(e-e)} = \sum_k D_k \frac{u^2}{v_e^2} \exp\left(-\frac{u^2}{v_e^2} \right), \tag{11}$$

where

$$D_k = \frac{|\tilde{b}_k|^2}{B_0^2} \frac{1}{2\pi^{1/2}|k_\parallel|}, \tag{12}$$

$u = \omega/k_\parallel$ and $\tilde{b}_k = \mathbf{k}\times\mathbf{b}_0 \cdot \mathbf{r} A_{\parallel\mathbf{k}}$. The convective part of the usual quasilinear heat flux does not appear in the LBTCI due to the cancellation referred to above. As suggested in Ref. 2, the conductive part of the energy moment survives the cancellation. However, this is true only for the perpendicular energy. Both the conductive and convective parts of the *parallel* energy moment are canceled by the drag. This outcome contradicts the assertions of Ref. 2. As noted, the presence of a conductive flux and absence of a convective flux mimics collisional transport, which, for like particles, yields a zero diffusivity and a nonzero thermal conductivity.

Assuming adiabatic ions ($u < v_i$), the ion components of Eq. (2) are given by

$$D_{\nabla n}^{(e-i)} = \sum_k 2D_k \frac{u^2}{v_i^2}\frac{\tilde{v}^2}{v_e^2}\left(1+\frac{\omega}{\omega_{*e}}\right)\left(1-\frac{k_\perp^2\rho_i^2}{2}\right) \times \exp\left(-\frac{u^2}{v_i^2}\right), \quad (13)$$

$$D_{\nabla T}^{(e-i)} = \sum_k 2D_k \frac{u^2}{v_i^2}\frac{\tilde{v}^2}{v_e^2}\left[\frac{u^2}{v_i^2}-\frac{1}{2}-\left(1+\frac{4u^2}{v_i^2}\right)\frac{k_\perp^2\rho_i^2}{8}\right] \times \exp\left(-\frac{u^2}{v_i^2}\right), \quad (14)$$

where $\tilde{v}^2 \equiv (\int v_\perp\, dv_\perp\, \tilde{h}_e)^{-1}\int v_\perp\, dv_\perp\, v_\perp^2 \tilde{h}_e \approx v_e^2$ is the perpendicular energy of electrons in the incoherent distribution and the lowest-order finite ion gyroradius corrections have been included. The ion components arise from the ion integrals $\int d^3v\, F_i$ and $\int d^3v\, v_\parallel F_i$ in quasineutrality and Ampère's law and are thus ambipolar constrained, as indicated by the ion velocity factor in Eq. (2). The ion terms describe wave-moderated electron–ion scattering. Though these expressions are nominally convective and conductive, the driving gradients are in the ion distribution. Therefore, these terms are not convective and conductive in the usual sense (electron gradient drives electron heat loss); rather, they are more akin to off-diagonal terms involving gradients of the opposite charge species. For MST, it is possible that u is as large as v_i making the hydrodynamic regime of interest. For $\nu_i < \omega$ (and $u > v_i$) weak collisions provide the necessary dissipation to produce transport. In this regime the diffusivities are

$$D_{\nabla n}^{(e-i)} = \sum_k \pi^{-1/2} D_k \frac{v_i}{u}\frac{\nu_i}{\omega}\frac{\tilde{v}^2}{v_e^2}\left(1+\frac{\omega}{\omega_{*e}}\right)\left(1-\frac{k_\perp^2\rho_i^2}{2}\right), \quad (15)$$

$$D_{\nabla T}^{(e-i)} = \sum_k \pi^{-1/2} D_k \frac{v_i}{u}\frac{\nu_i}{\omega}\frac{\tilde{v}^2}{v_e^2}\left(1-\frac{3k_\perp^2\rho_i^2}{2}\right). \quad (16)$$

The conductive heat flux [Eq. (14)] yields a heat pinch in the deeply adiabatic regime $u^2/v_i^2 \ll \frac{1}{2}$. For ω in the electron diamagnetic direction, this pinch is smaller than the outward convective flux [Eq. (13)], making the net flux outward. In the weakly adiabatic and hydrodynamic regimes $u^2/v_i^2 > \frac{1}{2}$, the conductive flux changes sign and becomes outward. The ion components of the electron heat flux are not completely general. In particular, magnetic drifts (grad B and curvature) have not been considered.

Evaluation of the heat flux [Eq. (10)] ultimately requires an assessment of the relative magnitudes of the electron and ion components. This, in turn, requires a consideration of the spectrum sums in the diffusivities. Because magnetic fluctuation-induced transport is produced by particles streaming along turbulent fields, the flux is critically sensitive to spectral variation in $k_\parallel$. In prior treatments, spectra that are peaked about $k_\parallel = 0$ with some width $\Delta k_\parallel$ have generally been assumed.[16] Such an assumption is valid near the rational surfaces of the modes that locally dominate the spectrum. It is not valid if the modes that locally dominate the spectrum are resonant at a distant rational surface. For a centrally peaked spectrum, the Rechester–Rosenbluth heat flux expression is recovered from Eq. (10). This is most easily seen for a spectrum that is flat out to $\Delta k_\parallel$ and zero thereafter. To facilitate evaluation, we take the continuous limit and convert the sum over $k_\parallel$ to an integral. From dimensional considerations, $\tilde{b}_k^2 = \tilde{b}^2/\Delta k_\parallel$, for $|k_\parallel| < \Delta k_\parallel$, where $\tilde{b}^2$ is the spectrum-averaged magnetic fluctuation level. With $\chi = 1/k_\parallel^2$, the expression for $D_{\nabla T}^{(e-e)}$ becomes

$$D_{\nabla T}^{(e-e)} = \int_{1/\Delta k_\parallel}^{\infty} d\chi\, \frac{\tilde{b}^2/B_0^2}{\Delta k_\parallel}\frac{1}{4\pi^{1/2}}\frac{\omega^2}{v_e^2}\exp\left(-\frac{\chi\omega^2}{v_e^2}\right) \approx \frac{\tilde{b}^2/B_0^2}{\Delta k_\parallel}\frac{1}{4\pi^{1/2}}, \quad (17)$$

when $v_e > \omega/\Delta k_\parallel$. Following the same procedure for the sums in Eqs. (13) and (14) then leads to the conclusion that the electron term dominates Eq. (10) by a factor proportional to the ratio (v_e/v_i). The resultant transport satisfies a Rechester–Rosenbluth expression.

Consider now a peaked spectrum that is shifted off $k_\parallel = 0$ by an amount $k_0 > \Delta k_\parallel/2$. This spectrum has virtually no power in the locally resonant modes for which $k_\parallel \approx 0$, but is dominated by modes resonant at remote rational surfaces. Such a spectrum could apply for a limited range of frequencies, one that dominates the heat flux, with fluctuations outside the range having $k_\parallel \approx 0$, as required to produce a stochastic field locally. As shown below, this is precisely the situation in MST. For a shifted spectrum that is flat, with width $\Delta k_\parallel$, the sums in Eqs. (11) and (13)–(16) can again be carried out without difficulty. Evaluating $D_{\nabla T}^{(e-e)}$ yields

$$D_{\nabla T}^{(e-e)} = \int_{(k_0+\Delta k_\parallel/2)^{-2}}^{(k_0-\Delta k_\parallel/2)^{-2}} d\chi\, \frac{\tilde{b}^2/B_0^2}{\Delta k_\parallel}\frac{1}{4\pi^{1/2}}\frac{\omega^2}{v_e^2}\exp\left(-\frac{\chi\omega^2}{v_e^2}\right) \approx \frac{\tilde{b}^2/B_0^2}{k_0}\frac{1}{2\pi^{1/2}}\frac{\omega^2}{v_e^2 k_0^2}\left(1-\frac{\Delta k_\parallel^2}{4k_0^2}\right)^{-2}, \quad (18)$$

where it has been assumed that all power lies in the adiabatic regime, $\omega/(k_0 \pm \Delta k_\parallel/2) < v_e$. The factor $(\omega^2/v_e^2 k_0^2)(1-\Delta k_\parallel^2/4k_0^2)^{-2}$ arises from the difference in the number of resonant particles at the extremes of the spectrum. For this spectrum the magnetic diffusivity for electron motion is smaller than the Rechester–Rosenbluth expression by the factor $(\omega/v_e k_0)^2$. Because the corresponding factor $(\omega/v_i k_0)^2$ also appears in the ion diffusivities, the ion terms are larger than the electron term. These factors reflect the number of particles of species j that are resonant with the collective mode. With both species adiabatic, the phase velocity ω/k_0 falls in the bulk of both distributions. Because the ion distribution is narrower, there are more resonant ions, and turbulent electron–ion scattering dominates the electron heat flux. Note that in this case, the heat loss is manifestly ambipolar.

IV. DISCUSSION

We now comment on Eqs. (11)–(18) as they pertain to the electron magnetic fluctuation-induced heat loss in MST.

(1) In the edge of MST, where the measurements reported in Sec. II were made, the magnetic fluctuation spec-

trum as a function of $k_\parallel$ is peaked well away from $k_\parallel=0$, with little power at $k_\parallel=0$. Since $\tilde{b}^2_{k_\parallel}$ is not directly measured, this spectrum structure must be inferred from $\tilde{b}^2_{m,n}$ (where m and n are the poloidal and toroidal mode numbers) and from the expression for $k_\parallel$ in the edge of a RFP. Expanding $B_{0\phi}(r)$ ($\ll B_{0\theta}$) in the region of the reversal layer,

$$k_\parallel(r,m,n)=\frac{n}{R}\left[r-r_s(m,n)\right]\left(\frac{1}{B_{0\theta}}\frac{dB_{0\phi}}{dr}\right)\Bigg|_{r=r_s(m,n)}, \qquad (19)$$

where $r_s(m,n)$ is the resonant surface for the m,n helicity. For the global tearing modes that dominate the spectrum, $k_\parallel$ is not close to zero because $r-r_s$ is large [we are interested primarily in the region $r\approx 0.8a$, while $r_s(m=1,\ n=5\text{–}8)$ is deep in the core]. The parallel wave number does, or course, approach zero when $r=r_s\approx 0.8a$. Using a Bessel function model for $B_{0\theta}(r)$ and $B_{0\phi}(r)$, this requires $n\gtrsim 50\text{–}70$. In this range the fluctuation power is down by two orders of magnitude. More critically, measurements of toroidal mode number versus frequency place fluctuations in this range at frequencies above 100 kHz. The cross-power spectrum (Fig. 1) indicates that fluctuations with frequencies above 20 kHz make virtually no contribution to transport. For $r=0.8a$, and with the power concentrated at $m=1$, $n=6$, the $k_\parallel$ spectrum peaks in the range $k_\parallel=1\text{–}2\ \text{m}^{-1}$ and falls to zero in a narrow band around this range. Under this circumstance, the spectrum is like that assumed in deriving Eq. (18). Consequently, the ion contribution to the flux dominates the electron component and the heat loss is ambipolar.

(2) Assuming that the frequencies of the dominant magnetic fluctuations in the plasma frame are in the range of measured frequencies (10–20 kHz), ω is somewhat larger than the diamagnetic frequency ω_{*e}. The convective ion component is therefore modestly larger (by a factor of ~ 6) than the conductive component, for comparable density and temperature gradient scale lengths. Of course, this conclusion must be regarded with caution because the frequency spectrum has rotation-induced Doppler shifts. However, it is quite possible that the frequency of the dominant modes, as measured in the plasma frame at $r=0.8a$ (where there is little rotation), is given primarily by the rotation rate at the resonant surfaces of the dominant modes. It also appears that the temperature is weaker than the density gradient, further favoring the convective component over the conductive component.

(3) For the frequency and wave number ranges presented above, the phase velocity $u=\omega/k_0$ is comparable to the ion thermal velocity, making the factor $\omega/v_i k_0$ close to unity. The ion diffusivity is thus close in magnitude to the Rechester–Rosenbluth diffusivity, while the flux carries an ion streaming factor.

(4) On the basis of inferred spectrum shapes, it is possible to predict the radial dependence of the heat flux in a RFP. Moving inward from the edge, the $k_\parallel$ spectrum shifts toward $k_\parallel=0$ as the distance to the resonant surfaces of the global tearing modes decreases. Approaching these surfaces, the spectrum first overlaps $k_\parallel=0$ and then peaks at $k_\parallel=0$. In this process, the heat flux goes from being ambipolar, with the loss rate fixed by an ion thermal velocity, to nonambipolar, with the rate governed by the electron thermal velocity. The magnitude of the heat flux therefore rises dramatically in moving from the edge into the core. This is consistent with observations, which indicate a sharp rise in heat flux as radius decreases. It is also consistent with the rather flat temperature profiles of the core region and confinement controlled at the edge. These qualitative statements are validated by a more quantitative analysis based on the central temperature response to sawtooth events, as seen by Thompson scattering. Using a Rechester–Rosenbluth expression with central values for the magnetic fluctuation amplitude, pressure, and gradient scale length, the temperature response is well fit using the electron thermal velocity.[17] This discussion may also have some bearing on magnetic fluctuation-induced transport in tokamaks. In tokamaks, it is generally assumed that the $k_\parallel$ spectrum either peaks about zero or has a significant $k_\parallel=0$ component. However, if the fluctuation energy is concentrated at low-order surfaces and these are sufficiently separated radially, it is possible that the heat flux makes a partial transition from being dominated by the electron term to being ambipolar constrained. This would result in regions of better confinement interspersed with regions of poor confinement, despite the absence of good flux surfaces. Recent observations on Continuous Current Tokamak[18] are consistent with such an effect.

Two points relating to the frequency dependence of the heat flux are also worth making. The first concerns the Lundquist number scaling of the flux. Normally it is assumed that the flux scaling is governed by the scaling of the power spectrum. However, when the $k_\parallel$ spectrum peaks away from $k_\parallel=0$, the flux depends on the frequency. It is conceivable that the frequency has some Lundquist number dependence. The second point is to note the isotope scaling of the heat flux. The thermal velocity dependence of Eqs. (15) and (16), in conjunction with velocity multiplier in Eq. (11), is somewhat unfavorable in its isotope scaling. However, the frequency likely has a favorable isotope scaling based on observed decreases of sawtooth frequencies in going from hydrogen to deuterium.

The points discussed above represent significant areas of plausible agreement between theory and experiment. This agreement cannot be expected for theories that ignore the nonlinear bunching of electrons. Clearly, more information is needed to determine the frequency of the tearing mode fluctuations in the plasma frame. This necessarily requires sorting out the frequency spectra of the dominant low n modes in relation to sawtoothing, rotation, diamagnetic effects, and aliasing from high n modes.

In summary, measurements of the magnetic fluctuation-induced electron heat flux in MST indicate that it is predominantly convective and its rate is governed by the ion thermal velocity. This result does not agree with common theoretical expectations that hold that electron heat loss is not subject to ambipolar constraints, allowing the loss rate to be governed by the electron thermal velocity and favoring conductive heat loss over convective heat loss. In this paper, we have proposed an explanation for the observations based on a proper accounting of the effects of nonlinear electron bunching. This leads in a natural way to ambipolar constraints.

Magnetic turbulence in MST appears to offer the first experimental evidence for such constraints in three-dimensional (3-D) magnetized plasmas. Theoretical expressions for the heat flux that include bunching are consistent with the experimental observations, within experimental uncertainties.

ACKNOWLEDGMENT

This work was supported by the U.S. Department of Energy.

[1] R. E. Waltz, Phys. Fluids **25**, 1269 (1982).
[2] A. A. Thoul, P. L. Similon, and R. N. Sudan, Phys. Rev. Lett. **59**, 1448 (1987).
[3] A. A. Thoul, P. L. Similon, and R. N. Sudan, Phys. Plasmas **1**, 601 (1994).
[4] F. W. Perkins, in *New Ideas in Tokamak Confinement*, edited by M. N. Rosenbluth (American Institute of Physics, New York, 1994), p. 259.
[5] G. Fiksel, S. C. Prager, W. Shen, and M. Stoneking, Phys. Rev. Lett. **72**, 1028 (1994).
[6] R. N. Dexter, D. W. Kerst, T. W. Lovell, S. C. Prager, and J. C. Sprott, Fusion Technol. **19**, 131 (1991).
[7] A. B. Rechester and M. N. Rosenbluth, Phys. Rev. Lett. **40**, 38 (1978).
[8] T. Boutros-Ghali and T. H. Dupree, Phys. Fluids **24**, 1839 (1981).
[9] P. W. Terry, P. H. Diamond, and T. S. Hahm, Phys. Rev. Lett. **57**, 1899 (1986); P. W. Terry, P. H. Diamond, and T. S. Hahm, Phys. Rev. Lett. **60**, 966 (1988).
[10] P. W. Terry and P. H. Diamond, Phys. Fluids B **2**, 1128 (1990).
[11] D. J. Den Hartog, A. F. Almagri, J. T. Chapman, H. Ji, S. C. Prager, J. S. Sarff, R. J. Fonck, and C. C. Hegna, Phys. Plasmas **2**, 2281 (1995).
[12] M. R. Stoneking, S. A. Hokin, S. C. Prager, G. Fiksel, H. Ji, and K. J. Den Hartog, Phys. Rev. Lett. **73**, 549 (1994).
[13] S. Ortolani and D. D. Schnack, *Magnetohydrodynamics of Plasma Relaxation* (World Scientific, Singapore, 1993).
[14] Y. L. Ho, Nucl. Fusion **31**, 341 (1991).
[15] J. S. Sarff, S. A. Hokin, H. Ji, S. C. Prager, and C. R. Sovinec, Phys. Rev. Lett. **72**, 3670 (1994).
[16] J. A. Krommes, C. Oberman, and R. G. Kleva, J. Plasma Phys. **30**, 11 (1983).
[17] M. Cekic, D. J. Den Hartog, M. R. Stoneking, J. S. Sarff, S. C. Prager, and P. W. Terry, Bull. Am. Phys. Soc. **40**, 1753 (1995).
[18] G. Fiksel, S. C. Prager, P. Pribyl, R. J. Taylor, and G. R. Tynan, Phys. Rev. Lett. **75**, 3866 (1995).